Effects of Confinement on Flame Spread in Microgravity

Yanjun Li[1] and Ya-Ting T. Liao[2]
Case Western Reserve University, Cleveland, OH, 44106, USA

Paul V. Ferkul[3] and Michael C. Johnston[3]
Universities Space Research Association, NASA Glenn Research Center, Cleveland, OH, 44135, USA

and

Charles Bunnell[4]
ZIN Technologies, Middleburg Heights, OH, 44130, USA

Solid fuel combustion experiments aboard the ISS examine the effects of confinement on a concurrent, purely-forced-flow flame spread in microgravity environment. The results for a thin, cotton-fiberglass-blended textile fabric fuel are presented. Flat baffles of differing materials are used to alter the radiative boundary conditions with transparent polycarbonate, black anodized aluminum (reflectance ~ 0), and highly polished aluminum (reflectance ~ 1). The baffles are parallel to the fuel sheet and placed symmetrically on each side. The inter-baffle distance is varied to change the boundary conditions for the flow. In all tests, samples are ignited at the upstream leading edge and allowed to burn to completion. Results show that the flame reaches a steady length and spread rate at low flow speeds (< 15 cm/s) for all tested inter-baffle distances. As the distance decreases, the flame length and spread rate first increase then decrease showing an optimal inter-baffle distance. For all baffle types, the flame either fails to ignite or extinguishes before reaching the end of the sample when the inter-baffle distance is too small (~ 1 cm). This is attributed to the reduction of oxygen supply to the flame zone and heat loss to the baffles. The results also show at the same inter-baffle distance, flame length and spread rate are highest for polished aluminum baffles, and lowest for transparent polycarbonate baffles. The differences are most prominent at intermediate tested baffle distances. While the radiative heat feedback from the baffles is expected to increase when the baffle distance decreases, the combustion is limited by the reduced oxygen supply. Near this limit, flame lengths and spread rates are similar for all baffle types.

I. Introduction

FIRE safety is of critical importance in aircraft and space vehicles due to limited options to suppress fires and the difficulty to evacuate. To address this, numerous experiments have been carried out to study how flames spread over solid materials in microgravity. These experiments used drop towers [1, 2], parabolic flights [3], sounding rockets [4], facilities aboard the International Space Station (ISS) [5, 6], and other space vehicles [7, 8]. The previous experiments focused on the effects of environmental conditions (e.g., oxygen percentages, pressure levels, flow velocities) and flow configurations (concurrent or opposed). They provided abundant data regarding the flame structure, flame spread rate, mechanisms for flame spread, and mechanisms for extinctions. For example, a previous NASA project, Burning and Suppression of Solids (BASS) examined the burning processes of various materials (e.g., thin cotton-fiberglass based fabrics, Nomex, Ultem, PMMA slabs, rods, and spheres) in concurrent and opposed flows using a small flow duct (height: 7.8 cm) operated in the Microgravity Science Glovebox (MSG) aboard the ISS [5, 6]. For the tested cotton-fiberglass fabric samples (referred to as SIBAL), steady flame spread was observed in low-speed concurrent flows (~20 cm/s). The flame length and spread rate increased with flow velocity and ambient oxygen

[1] PhD Candidate, Department of Mechanical and Aerospace Engineering, 10900 Euclid Avenue.
[2] Assistant Professor, Department of Mechanical and Aerospace Engineering, 10900 Euclid Avenue.
[3] Staff Scientist, Low Gravity Exploration Technology, NASA Glenn Research Center, MS 110-3.
[4] Payload Developer, Space Experiments Department, ZIN Technologies, Inc.

percentage up to the hardware limitation of 22% volume fraction oxygen. A low-speed quenching velocity was also identified and shown to decrease when the oxygen percentage increased. In another NASA-led project Saffire, large samples of the same cotton-fiberglass fabric were burned in a large flow duct (height: 41 cm) inside the pressurized cabin of the unmanned Cygnus ISS resupply vehicle [7]. While steady flame spread was also observed, the flame spread rates at the steady state in Saffire were significantly lower than those obtained in BASS even at the same oxygen percentage and flow rate. The different spread rates were suspected to be due to the different confined conditions introduced by the large and small flow ducts used in these two experiments.

Similar phenomenon was reported in numerical studies [9, 10, 11]. Shih and T'ien used a two-dimensional steady Computational Fluid Dynamics (CFD) combustion model to study concurrent-flow flame spread over thin solid samples in a flow duct in microgravity. [10, 11]. Their results show that, when the flow duct height decreases, the flame length and flame spread rate first increased and then decreased. Flow chimney effect, restriction of oxygen supply, and heat loss to the duct walls were identified as competing factors that resulted in the observed non-monotonic trend of the flame spread rate. Furthermore, when the radiation reflection from the duct walls was considered in the model, converged solutions were not achieved for some simulated duct heights. It is suspected that the flame may be continually growing in these confined conditions and this transient process cannot be captured by a pseudo steady time independent model. Li et al [9, 11] conducted three-dimensional transient numerical study and considered the geometry of the BASS experiments. In their work, the duct height was varied between 1 cm and 9 cm to investigate the effects of the flow confinement on flame spread. The results predicted that the optimal duct height for fastest flame spread in a 10 cm/s air flow was 4.0 cm. Above this optimal duct height, the flow confinement affects the flame spread process mainly through the chimney effect as the heated gases expand. The flame spread rate has an approximately linear dependency on the inverse of the duct height [11] in this regime. Below the optimal duct height, the flame spread rate is proportional to the oxygen supply to the combustion zone and the spread rate is approximately linearly proportional to the duct height [11].

In normal gravity, previous experiments also showed that fires in confined spaces (e.g., parallel panels, channels) can be longer and spread faster compared to fires in open spaces [12, 13]. Shih and Wu [12] performed upward flame spread experiments over parallel thin paper sheets. When the distance between the paper sheets is larger than 10 cm, fire behavior is similar to that of one single sheet. As the separation distance between the paper sheets decreases, the adjacent flames begin to interact with each other and flame spread rate increases. It was concluded that both the chimney effect and the radiation interactions between the adjacent flames and samples intensify the fires. However, when the separation distance is further reduced, flames between parallel samples suffer from oxygen depletion and the flame spread rate decreases.

In microgravity, to the authors' best knowledge, there were no experiments that specifically investigate the effects of confinement on fire behavior. In this new ISS project (referred to as Confined Combustion), the BASS hardware is refurbished and modified to allow different levels of flow confinement and different radiative wall reflection. The aerodynamic and radiative interactions between a flame and its surrounding walls and the fate of the flame (no ignition, growing flame, steady flame, or extinction) are explored systematically for various confined conditions. The ultimate goal is to provide guidance for future structural designs and improve fire safety codes for both space and Earth applications. This paper presents the concept and some initial data from the microgravity experiments.

II. Experimental Setup

The experimental setup is shown in Fig. 1. The experiment is based on the existing flow duct hardware from BASS [5, 6]. The flow duct is 20 cm long and has a square cross-section 7.6 cm × 7.6 cm. It is capable of providing flow up to 55 cm/s. The duct operates in the Microgravity Science Glovebox (MSG) used for work volume isolation aboard ISS. Along with ISS environmental sensor data, an O_2 sensor (Quantek model 201 accuracy +/-2% of reading) is installed in the MSG to monitor the oxygen consumption during each test. A high-resolution video camera is used to record the burning events from the top window of the flow duct. The spatial resolution and the frame rate of the video recordings are 12.5 pixels/mm (or 0.08 mm/ pixel) and 24 frames per second (or ~ 42 ms/frame) respectively. The camera is set to auto adjust for white balance, exposure, and digital gain. An ISS laboratory camera downlink was occasionally used for a secondary view through the MSG front window.

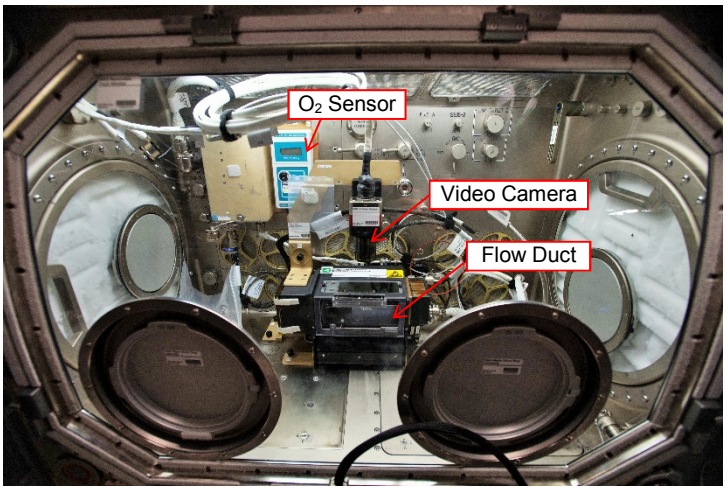

Figure 1. Experimental setup in the Microgravity Science Gloves aboard the International Space Station.

In this work, a new baffle/sample system is developed (Fig. 2). Similar to BASS, each sample is held in position sandwiched between two stainless steel sample frames with black oxide surface treatment (Fig. 2a). The sample frame is 13.8 cm long and 6.1 cm wide and the exposed sample surface is 10 cm long and 2.2 cm wide. A 29-AWG Kanthal hotwire with resistance ~ 1 Ω is located at the leading edge of the sample to serve as the igniter. The sample frame is then placed at the center position of a mounting system, together with two parallel flat baffles (Fig. 2b), one on each side of the sample. The dimensions of the baffles are the same as the sample frame (13.8 cm by 6.1 cm). The mounting system consists of a series of 5mm spacers. By controlling the number of spacers between the baffles and the sample, different levels of flame confinement are achieved. The variation of the inter-baffle distance in the flow direction is measured to be within 3% in all cases. A transparent top window is custom-designed to be retrofitted to the BASS flow duct and the baffle/sample assembly is magnetically attached to a mount integrated with the top window. This new system was designed in a way that the sample is positioned exactly in the middle of the flow duct when the baffle/sample assembly is mounted on the top window.

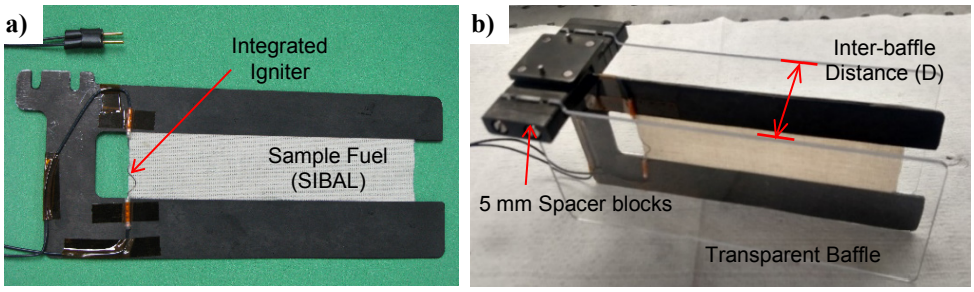

Figure 2. a) Sample frame with fuel and igniter. b) Assembly of the sample/baffle carrier, sample frame, and two parallel transparent baffles. The distance of the fuel to either baffle is D/2.

In Confined Combustion, tested sample materials include the SIBAL fabric (75% cotton, 25% fiberglass, see Fig. 2a) previously tested in BASS [5] and 1mm-thick cast PMMA slabs. In this paper, only selected data from the SIBAL fuel tests are presented.

Three types of baffles are used: transparent polycarbonate, black anodized aluminum, and reflective, highly-polished aluminum (Fig. 3). The surface properties of each baffle are characterized on the ground prior to the experiments. For the black and reflective baffles, the specular reflection gloss levels are tested using Konica Minolta Multi Gloss 268A glossmeter at three measurement angles, 20°/60°/85°. The values for the reflective baffles are 1300,

670, and 130 GU (gloss units) at the three tested angles respectively, and the values for the black baffles are 0, 0.3, and 1.3 GU respectively. Note that these reflectance measurements only characterize visible light reflectance.

The visibly transparent baffles are made from 1.6-mm-thick general purpose clear polycarbonate. The transparency is tested using a 5,500K color temperature white light LED and a UV-enhanced silicon photodiode. The baffle is inserted between the light source and the broadband photodetector. Baseline tests are also performed without any baffles. The differences between the measurements with and without baffles are used to determine the transmittance of the baffles. This measurement is repeated three times and the average transmittance is 92.5% for the polycarbonate baffles. It should be noted that the tested spectrum range is mainly in the visible light wavelengths. The flame radiation in the infrared range (e.g., at wavelength 2,500~3,000 nm from H_2O and CO_2, and at ~4,400 nm from CO_2 [14]) may transmit the baffles at lower rates. Based on the manufacture's data [15], the transmittance for a 1 mm-thick polycarbonate remains fairly constant at ~90% for wavelength 400~1,600 nm, drops to ~ 40% at 1,650nm, and increases back to 80% at 1,750~ 1,950nm. Further testing is warrant to obtain information of the transmittance at higher wavelengths.

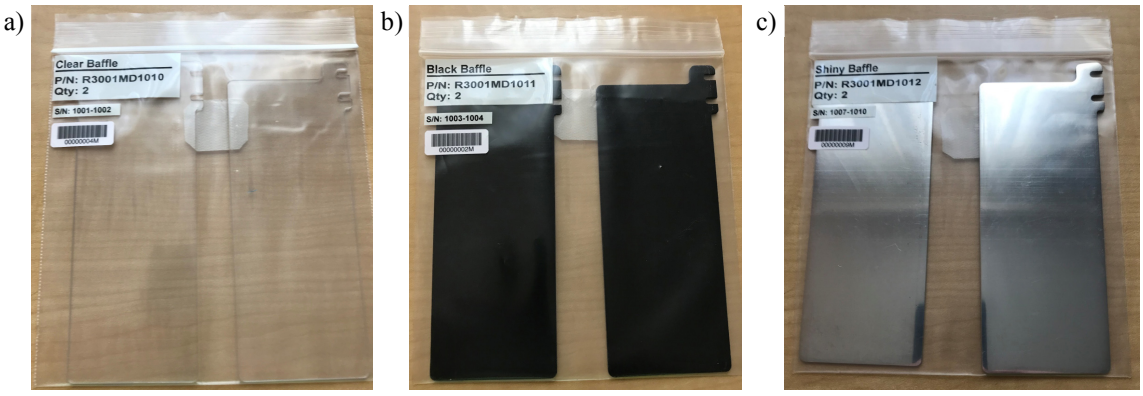

Figure 3. Three types of baffles. a) Transparent polycarbonate. b) Anodized black aluminum. c) Polished aluminum.

During the experiment operations, real time space to ground communication and live video downlink is established between ISS crew and the science team in the Tele-Science Communications Center at NASA Glenn Research Center. In all tests, the pressure and oxygen percentage in the MSG remain constant at ISS ambient values of 1.0 atm and ~22% respectively. The daily variation of oxygen concentration in MSG is between 21.3% and 22.9%. Imposed flow velocities range from 5 – 28 cm/s. Preflight flow calibration was performed at various inter-baffle distances (30, 40, 50 mm) and at three different streamwise locations (near the entry, at the center, and near the exit of the duct). The results indicated that the flow rate between the baffles decreases slightly when the baffle distance decreases. For 7 cm/s imposed flow, the flow rate decreases by ~28% when the inter-baffle distance decreases from 50 mm to 30mm. The flow is fairly uniform in the streamwise direction with variation less than 10 % from the mean value.

Note that the width of the baffle/sample assembly (6.1 cm) is narrower than the width of the flow duct (7.8 cm). Small gaps (~ 0.8 cm) are present between the edge of the sample frame/baffles and the duct wall (or the duct window). Previous numerical study predicted that the flow can be diverted away from the inter-baffle space (where friction occurs on baffles and sample surfaces) to the side gaps [11], especially when the baffle distance is small (e.g., D = 1 cm). This effect contributes to the lower measured flow in the inter-baffle space when the baffle distance is reduced. Also note that, as shown in Fig. 2a, the sample frame on the spacer side (top side in the figure) is slightly narrower (by ~ 0.3 cm) than the sample frame on the other side. This results in a slightly larger side gap on the top edge of the sample/baffle assembly, compared with the bottom edge. However, this slightly unsymmetrical geometry of the sample/baffle assembly is expected to have minimal effects (if any) on the flame as the flame was observed to reside at the center of the sample frame and away from both side gaps in all tests.

The spacer blocks may also disturb the flow. Each of the blocks is around 0.7 cm tall. The Reynold's number based on this block height for the tested imposed flow speeds range from 24 – 132. While flow recirculation might occur in the region immediately downstream to the blocks, the flow disturbance does not seem to have a significant effect on the flame. In all tests, both the top view and the secondary front-view images (if available) did not show flame oscillations or consistent non-symmetries during the entire burning event.

After the flow is established, ignition current is powered on and lasts until the sample ignites and an established flame is observed. The ignition and flame development processes are monitored in real time and recorded using a video camera through the flow duct top window (Fig. 1). Post-burn sample images are also obtained.
When the imposed flow velocity is less than 15 cm/s, steady state flame spread is observed for most of the tests. When the flow velocity is higher than 15cm/s, the flame continually grows and does not reach a steady state except when the inter-baffle distance is small (< 3 cm). Note that this observation might be specific to the tested sample length. It is possible that the flame will eventually reach a steady state at these conditions if given a longer sample length. This paper focuses on the cases where steady state is reached and discusses how the confinement affects the steady state flame attributes.

III. Results

A. Flame Development Process

When the imposed flow is less than 15 cm/s, the flame reaches a steady length and spread rate in most cases. The typical process of the transient flame development leading to the steady state is shown in Fig. 4 using a representative case. In this case, the sample is placed between two black baffles with 5.0 cm inter-baffle distance (outside of the cropped frame). The imposed flow velocity is 5 cm/s. Note that these images showing the edge view of the fuel (the camera line-of-sight is parallel to the sample surface) are taken through the top window of the flow duct (see Fig. 1).

The igniter is bright in initial frames illuminating the interior of the flow duct. After the igniter is de-energized and after a short growth period, the flame reaches a limiting length and steady spread rate. The flame exhibits clearly two layers of different colors: a thinner yellow layer of soot nearer to the sample surface and a thicker blue layer nearer to the two baffles. At the end of the test, the flame fronts reach the downstream open end of the sample and merge into a single flame front. Shortly after that, the sample is fully consumed and the flame quenches.

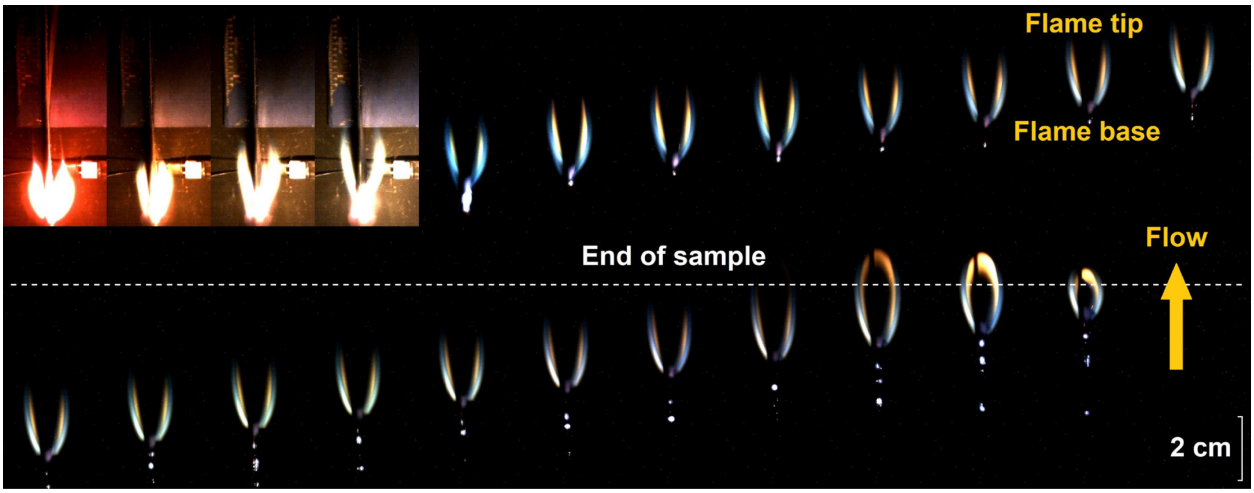

Figure 4. Transient flame growth process. Imposed flow is upward at 5 cm/s. Confined conditions: black anodized aluminum baffles with 5.0 cm inter-baffle distance. Ignition is at upper left and images are 2.4 s apart.

To quantify the flame development process, a video analysis computer code was developed to track the downstream flame tip and the upstream flame base positions (see Fig. 4). The result is shown in Fig. 5. Flame spread rate is taken as the slope of the linear least-squares curve fit through the flame tip and flame base data in the center region of the sample (between 4-7 cm) to avoid flame growth period and end effects. Flame length is taken as the average of the flame tip minus base positions in the same time duration.

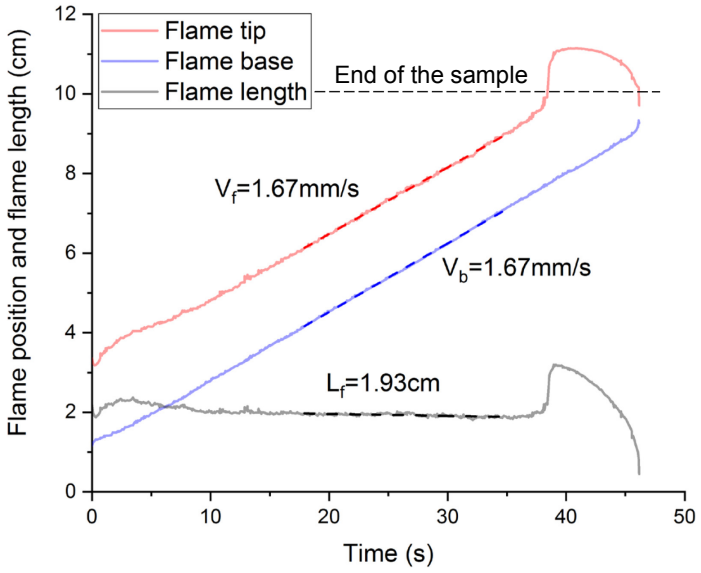

Figure 5. Flame positions versus time (time = 0 is defined when the ignitor is off). Imposed flow velocity: 5 cm/s. Confined conditions: black baffles with 5.0 cm inter-baffle distance. The dashed lines show the linear curve fits at the steady state condition.

Figures 4 and 5 show that near the end of the test, when the flame tip reaches the downstream open end of the sample, the flame tip accelerates, flame suddenly lengthens, and the left and right flames merge at the downstream end. Several factors may contribute to this. When the flame spreads along the fuel surface, the gaseous fuel pyrolysate needs to diffuse across the flow viscous boundary layer to meet with the oxygen in the flow stream. Thus the flame profile resembles the shape of the flow boundary layer [1]. At the downstream edge of sample, the boundary layer breaks due to absence of the solid fuel. Consequently, the gaseous fuel and hence the reaction zone from each side of the sample can join up. The sudden removal of the no-slip boundary condition also leads to increased flow speed near the center plane downstream to the sample fuel. Furthermore, the baffles ends near this location (see Fig. 2b). The downstream portion of the flame is no longer subjected to the confinement (no oxygen limitation and conductive heat loss to the baffles). The higher flow speed, additional oxygen supply, and reduced heat loss are suspected to contribute to the acceleration of the flame tip near the end of the test.

B. Effects of Flow Confinement

The flame profiles at different inter-baffle distances (and with no baffles) are compared in Fig. 6 at the same imposed flow speed of 7 cm/s. When the confinement varies from no baffles (the full duct width, equivalent to D = 7.6 cm) to the most confined case (D = 2.0 cm), flame length first increases and then decreases. The maximum flame length occurs at around D = 4.0 cm. When the inter-baffle distance further decreases to D = 1.0 cm, the flame quenches immediately after ignition energy is removed. Post-burn sample indicated that the flame never spread past the ignition wire (the sample burn length is less than 0.8 cm).

Note that in the case with no baffles, the sample was installed on the sample carrier (Fig. 2b) alone. The two sides of the sample were exposed directly to the interior of the flow duct (right side in Fig. 6) and to the front window (left side) respectively. The interior of the flow duct is painted black and its radiation property, although not measured, is expected to be close to a black surface. The front window was made of visibly transparent polycarbonate.

Also note that when the flame is small and weak at very small inter-baffle distances (e.g., D = 2.0 cm), the camera is struggling with white balance and the videos show unrealistic colors of the flames (see Fig. 6). The apparent colors would change between one video frame and the next. However, the ISS crew reported true flame color during the burns to confirm/correct the video displayed.

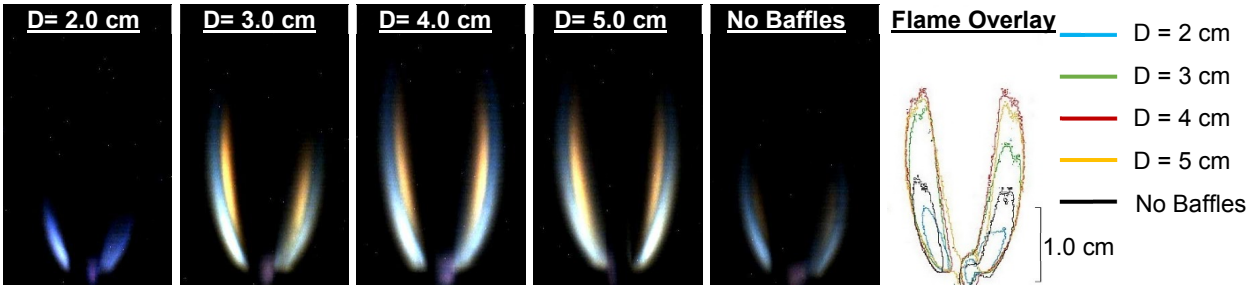

Figure 6. [Left] Comparisons of steady flame profiles for different flow confined conditions. Baffle types (if used): black anodized aluminum baffles. Imposed flow velocity: 7 cm/s. [Right] Overlay of tracked flame outer edge for all five tests. In the case with no baffles, the flame is between a black duct wall (right side in the figure) and a transparent polycarbonate window (left side in the figure).

The flame spread rates and flame lengths at different inter-baffle distances are compared in Fig. 7. The error bars denote the 95% confidence intervals of the measurements. Both flame characteristics exhibit non-monotonic trends when the inter-baffle distance decreases. When the confinement increases from D = 7.6 cm (no baffle case) to D = 5.0 cm, the flame spread rate increases by a factor of ~1.5 for the black anodized aluminum baffles. This increase is inversely proportional to the reduction of the cross-section area available for the thermal expansion ($V_f \sim 1/D$), consistent with the prediction of Li et al. [9]. This implies that the flow acceleration during combustion thermal expansion is responsible for the increased flame spread rate in this confined condition regime. For the reflective highly polished aluminum baffles, the increases in spread rate and flame length are even higher due to the additional radiative heat feedback reflected from the baffles. As predicted by Li et al. [9], the optimal inter-baffle distance for the flame spread occurs at D = 4.0 cm. The spread rate and flame length reach the maximum values for all baffle types. Below this inter-baffle distance, the flame spread rate decreases with the inter-baffle distance due to oxygen starvation and conductive heat loss to the baffles [9]. Compared to the linear dependency on the duct height as predicted by Li et al, the spread rate decreases faster when the inter-baffle distance decreases. In the experiments, it is possible that some flow is diverted to the extra-baffle regions (i.e., outside the baffles) due to the pressure buildup between the two baffles near the flame, an unintended limitation of the retrofit to the BASS duct. As a result, the flow that enters the inter-baffle region may be lower than the imposed flow velocity especially when the baffles are close. At D = 1.0 cm, ignition was not achieved for any baffle types.

In the previous BASS experiment, flame spread rate was measured for the same sample material at similar environmental conditions (1atm, 21% O_2) and with a slightly lower concurrent flow rate (5 cm/s). Compared with the case with no baffles in this work, the spread rate in previous BASS is ~ 42% higher. This difference in flame spread rates might be due to a combination of various reasons, one being the different sample card widths used in previous and current tests (3.6 cm vs 6.1cm respectively). While a wider sample card may introduce a faster flow that the sample encounters [11], this effect is only prominent when the duct height is small (close to the flow boundary layer thickness). The wider sample card used in this work is likely to introduce more heat loss and to reduce side oxygen transport to the combustion zone, both of which weaken the flame. In addition, there were other hardware differences between the previous BASS and current work: the sample orientation was rotated 90-degrees in the duct and the sample holder mechanism was changed.

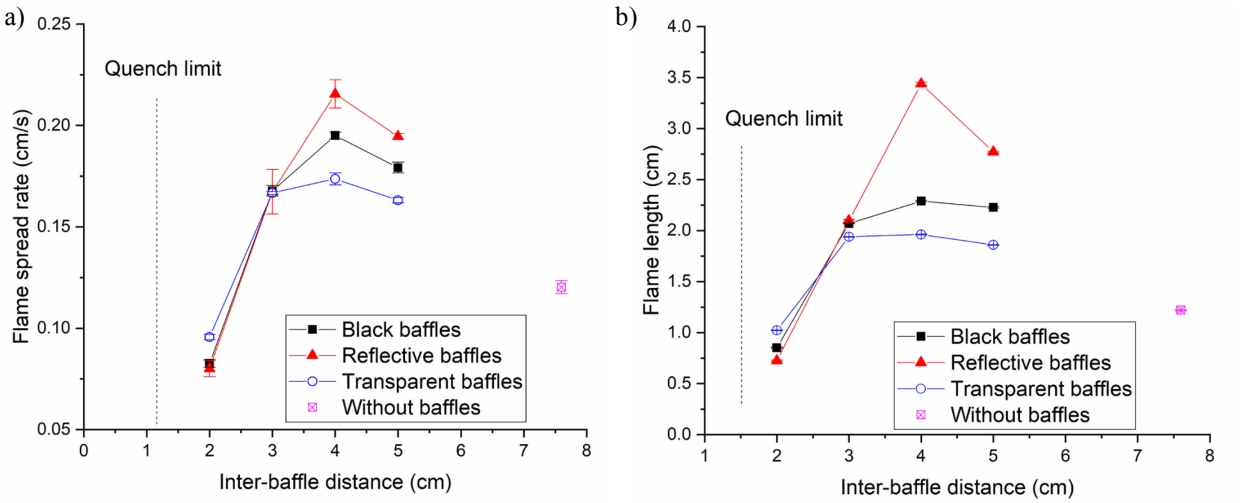

Figure 7. Flame spread rates and flame length at different inter-baffle distances. Imposed flow velocity: 7 cm/s.

C. Effects of Radiation Feedback

The flame profiles for different baffles are compared in Fig. 8. In these cases, the inter-baffle distances are 4.0 cm and the imposed flow velocity is 7 cm/s. Among the three cases, flame is significantly longer when the reflective baffles are used, as expected. During the burning process, a portion of the combustion heat is lost to the environment through radiation. The reflective baffles help to re-direct radiation back to the sample and the gaseous flame. On the other hand, a significantly higher portion of radiation penetrates or is absorbed by the transparent polycarbonate and black anodized aluminum baffles. Compared with the transparent baffles, the flame is slightly longer for the black baffles. During the burning process, temperature of the baffles increases thus more energy is emitted through surface radiation. The longer flame observed for the black baffles is likely due to the combination of a slightly higher radiation reflection and emission than transparent baffles.

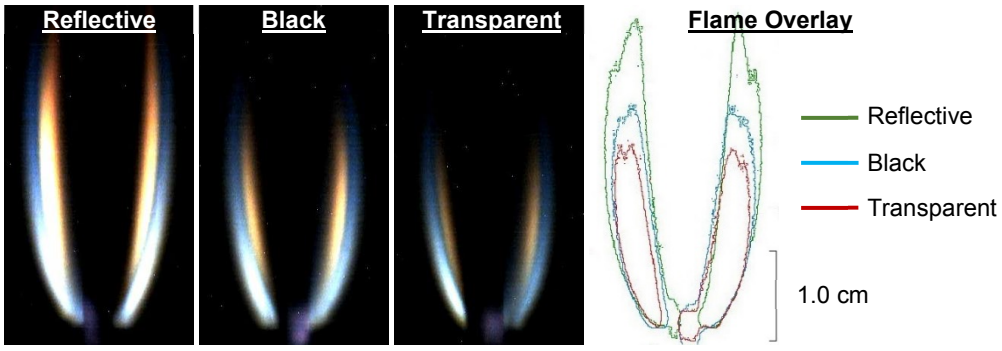

Figure 8: [Left] Comparisons of steady flame profiles between different baffle types. Baffle distance D = 4.0 cm. Imposed flow velocity: 7 cm/s. [Right] Overlay of tracked flame outer edge for all three tests.

The flame lengths and spread rates for different baffle types are compared in Fig. 7. It is noticed that at small inter-baffle distances (e.g., D < 3.0 cm), the flame spread rates for black and reflective baffles are similar but are different from those for transparent baffles. To further compare the differences caused by the baffle types, the ratios of the spread rates of the reflective and black baffles to the spread rate of the transparent baffles are shown in Fig. 9.

In general, the additional radiation feedback from the reflective baffle results in a higher flame spread rate compared with the black and transparent baffles. This effect is most prominent near the optimal inter-baffle distance,

D = 4.0 cm. At small baffle distances (e.g., D = 3.0 cm), the flame spread rates for different baffles are almost identical. This further suggests that at these confined conditions, the combustion is limited by the oxygen supplied to the inter-baffle region.

Note that at the minimum inter-baffle distance for which a flame spreads, D = 2.0 cm, the flame spread rate for the transparent baffles is slightly higher than other baffle types. This indicates that at this inter-baffle distance, the flame is close enough to the baffles such that conductive heat loss contributes to the decrease of the flame spread rate [9, 10]. Compared with the polycarbonate, the polished and anodized aluminum baffles have significantly larger thermal conductivity (200 vs. 0.2 W/m/K) and larger volumetric heat capacity ($\rho \cdot C_p \sim 2.46$ vs. 1.44 J/cm^3/K), and are therefore expected to introduce more heat loss from the flame zone.

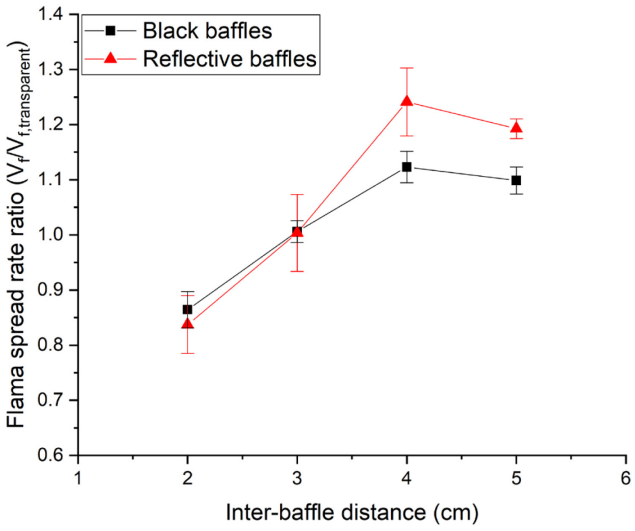

Figure 9. Comparisons of flame spread rate between different baffle types. The spread rate of transparent baffles is used as reference and its value in this plot is unity at all inter-baffle distances.

IV. Conclusion

A series of concurrent-flow flame spread experiments were performed in purely-forced concurrent flow in microgravity to study the effects of confinement on the burning characteristics of solid materials. Thin cotton-fiberglass blend fabrics were burned in a small flow duct in the Microgravity Science Glovebox (MSG) aboard the ISS. The imposed flow velocities ranged from 5 to 25 cm/s. Confinement is introduced using two baffles with adjustable distance between 1 and 5 cm installed parallel to the sample, one on each side. Three types of baffles: black anodized aluminum, reflective highly-polished aluminum, and transparent polycarbonate were used to simulate different radiative boundary conditions from the surrounding walls. The main findings are as follows:

1. For all tested flow velocities and baffle types, there exists a quenching inter-baffle distance below which the flame failed to spread.
2. When the imposed flow velocity is larger than 15 cm/s, the flame continually grows throughout the test (in the limited sample size available) except when the baffle distance is near the quenching distance.
3. For cases where steady flame spread was observed, the flow confinement has non-monotonic effects on the burning characteristics and there exists an optimal inter-baffle distance for flame length and spread rate (4.0 cm in this work). Above this optimal distance, the confinement affects the burning through the thermal expansion during combustion, which accelerates the flow and enhances the conductive heat feedback to the sample. This results in a higher flame spread rate. When the inter-baffle distance is smaller than the optimal distance, the flame suffers from the oxygen starvation and additional heat loss to the adjacent baffles. These weaken the flame and decrease the flame spread rate.
4. The reflective highly-polished aluminum baffles in general have the strongest flame (highest spread rate and longest length) and the transparent polycarbonate baffles have the weakest flames. This effect is most

prominent near the optimal inter-baffle distance. The trend reverses at quenching for small inter-baffle distances as the transparent baffles conduct the least heat away from the flame among the three baffle types.

Acknowledgments

This research is co-sponsored by the National Science Foundation and Center for the Advancement of Science in Space (CASIS) under grant number CBET-1740478. Hardware modifications for Confined Combustion and the original BASS hardware were performed by ZIN Technologies. The science team received tremendous support during operations from NASA Glenn Research Center, Marshall Spaceflight Center, and ZIN Technologies, and especially Emily Griffin, Steve Lawn, Russell Valentine, Beth Curtis, Chris Rogers, Wendell Booth, Michael Hall, and the Microgravity Science Glovebox team. We would also like to express our immense appreciation to our lab partners in space, ISS crew members Christina Koch, Jessica Meir, Andrew Morgan, and Luca Parmitano for supporting and conducting the microgravity experiments aboard the ISS.

References

[1] A. Vetturini, W. Cui, Y.-T. T. Liao, S. Olson and P. Ferkul, "Flame Spread Over Ultra-thin Solids: Effect of Area Density and Concurrent-Opposed Spread Reversal Phenomenon," *Fire Technology,* vol. 56, p. 91–111, 2020.

[2] S. L. Olson, P. V. Ferkul and J. S. T'ien, "Near-limit flame spread over a thin solid fuel in microgravity," *Symposium (International) on Combustion,* vol. 22, no. 1, pp. 1213-1222, 1989.

[3] A. F. Osorio, K. Mizutani, C. Fernandez-Pello and O. Fujita, "Microgravity flammability limits of ETFE insulated wires exposed to external radiation," *Proceedings of the Combustion Institute,* vol. 35, no. 3, pp. 2683-2689, 2015.

[4] H. D. Ross, "Basics of Microgravity Combustion," in *Microgravity Combustion: Fire in Free Fall*, London, UK, Academic press, 2011, pp. 22-23.

[5] X. Zhao, Y.-T. T. Liao, M. C. Johnston, J. S. T'ien, P. V. Ferkul and S. L. Olson, "Concurrent flame growth, spread, and quenching over composite fabric samples in low speed purely forced flow in microgravity," *Proceedings of the Combustion Institute,* vol. 36, pp. 2971-2978, 2017.

[6] P. V. Ferkul, S. L. Olson, F. Takahashi, M. Endo, M. C. Johnston and J. S. T'ien, *Thickness and Fuel Preheating Effects on Material Flammability in Microgravity from the BASS Experiment,* Orlando, USA: 29th Annual Meeting of the American Society for Gravitational and Space Research, 2013.

[7] D. L. Urban, P. Ferkul, S. Olson, G. Ruff, J. Easton, J. S. T'ien, Y.-T. T. Liao, C. Li, C. Fernandez-Pello, J. Torero, G. Legros, C. Eigenbrod, N. Smirnov, O. Fujita, S. Rouvreau, B. Toth and G. Jomaas, "Flame spread: Effects of microgravity and scale," *Combustion and Flame,* vol. 199, pp. 168-182, 2019.

[8] C. Li, Y.-T. T. Liao, J. S. T'ien, D. L. Urban, P. Ferkul, S. Olson, G. A. Ruff and J. Easton, "Transient flame growth and spread processes over a large solid fabric in concurrent low-speed flows in microgravity – Model versus experiment," *Proceedings of the Combustion Institute,* pp. 4163-4171, 2018.

[9] Y. Li, Y. Liao and P. Ferkul, "Concurrent-Flow Flame Spread Over a Thin Solid in a Narrow Confined Space in Microgravity," in *International Mechanical Engineering Congress & Exposition*, Salt Lake City, USA, 2019.

[10] H.-Y. Shih and J. S. T'ien, "Modeling Wall Influence on Solid-Fuel Flame Spread in a Flow Tunnel," in *35th Aerospace Science Meeting & Exhibit* , Reno, NV, 1997.

[11] Y. Li, Y.-T. T. Liao and P. Ferkul, "Numerical study of the effects of confinement on concurrent-flow flame spread in microgravity," *Journal of Heat Transfer,* p. Under review, 2020.

[12] H.-Y. Shih and H.-C. Wu, "An Experimental Study of Upward Flame Spread and Interactions Over Multiple Solid Fuels," *Journal of Fire Science,* vol. 26, no. 5, pp. 435-453, 2008.

[13] B. Comas, A. Carmona and T. Pujol, "Experimental study of the channel effect on the flame spread over thin solid fuels," *Fire Safety Journal,* vol. 71, pp. 162-173, 2015.

[14] E. K. Plyler and C. J. Humphreys, "Infrared Emission Spectra of Flames," *Journal of Research of the National Bure au of Standards,* vol. 40, pp. 449-456, 1948.

[15] Covestro, "Optical properties of Makrolon and Apec," Covestro Deutschland AG, 2017.